Predict and Prejudice: Classification of compact objects and model comparison using EOS knowledge

Hauke Koehn, **Thibeau Wouters**, Henrik Rose, Peter T. H. Pang, Rahul Somasundaram, Ingo Tews, and Tim Dietrich

t.r.i.wouters@uu.nl

Extreme Matter call 17/06/2024

Utrecht University

Nikhef

Overview

Our paper has several parts:

- Adding new NICER observation of PSR J0437-4715 (TBA)
- Classification of recent lower mass gap objects:
  - PSR J0514-4002E companion
  - GW230529 primary [1] (**main focus of this talk**)
- Model selection:
  - Comparison of NICER results for PSR J0030+0451
  - Comparison of symmetry energy measurements

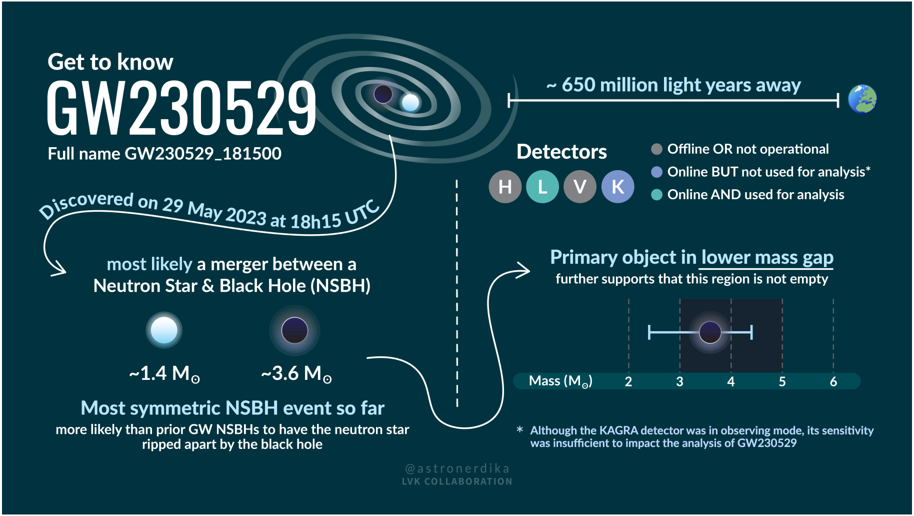

Credit: Shanika Galaudage

Methods – EOS constraints with NMMA

NMMA [2] compiled sets of EOS constraints [3]:

- Nuclear theory and experiments
- Radio observations pulsars, NICER, bursters, X-ray binaries
- GW170817 + EM counterparts & postmerger remnant

NMMA

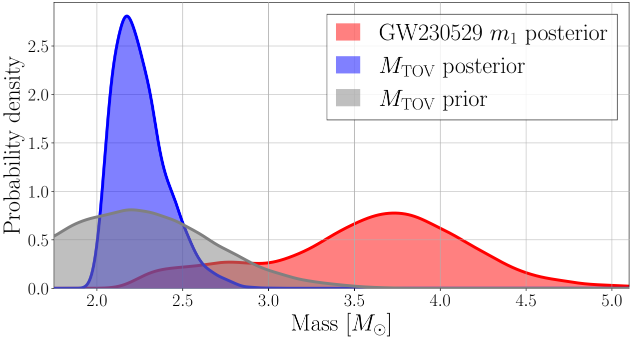

Methods – EOS constraint sets

Table 1: Overview on the constraints contained within the three different constraint sets.

Set	Label	Description
High confidence	1	Chiral EFT, pQCD, heavy radio pulsars, NICER J0740+6620, NICER J0030+0451, (NICER J0437-4715), GW170817
More vigorous	2	Set 1, Black Widow J0952-0607, heavy ion-collisions, qLMXBs, GW170817+KN+GRB afterglow, CREX, PREX-II, Burster 4U 1702-429, Burster J1808.8-3658, GW170817 postmerger
Aggressive	3	Same as set 2, but for the remnant of GW170817 a hypermassive neutron star above the Kepler limit is assumed

Methods – Classification of compact objects

NMMA sets of constraints $\mathcal{D}$ give posteriors on M_{TOV}.
Compare this against GW230529's properties:

- Probability of primary being a neutron star: $P(NS)$:

$$P(\mathsf{NS}) = \int \mathrm{d}M_{\mathsf{TOV}} \int_0^{M_{\mathsf{TOV}}} \mathrm{d}m_1 \; P(M_{\mathsf{TOV}}|\mathcal{D}) P(m_1).$$

- Spinning neutron stars can have higher masses: $M_{\max}(\mathrm{EOS}, \chi_1)$:

$$P(\mathsf{NS}) = \int \mathrm{d}M_{\max} \int_0^{M_{\max}} \mathrm{d}m_1 \int_0^1 \mathrm{d}\chi_1 \; P(M_{\max}|\mathcal{D}, \chi_1) P(m_1, \chi_1) \, .$$

- Use universal relation from Breu and Rezzolla for $M_{\max}$ [4]

Results – Classification of GW230529 primary

- Set 1 and without spin: agreement with LVK results [1].
- Spin + PDB raise $P(NS)$ to $\sim 17\%$.
- Set 3 ("aggressive") drastically reduces $P(NS)$.

		Set 1	Set 2	Set 3
default prior	w/o spin	1.6%	1.3%	0.02%
	w/ spin	3.9%	3.9%	0.82%
PDB prior	w/o spin	8.1%	6.9%	0.36%
	w/ spin	17%	17%	1.7%

(PDB: Powerlaw + Dip + Break population model)

Other results – PSR J0514-4002E

Binary MSP system observed by MeerKAT, with companion mass $m_c = 2.35^{+0.20}_{-0.18}\,M_\odot$ [5]. We use several priors:

- Constrain pulsar mass above $1.17 M_\odot$
- Isotropic prior
- Prior informed by galactic population

The companion is most likely a black hole.

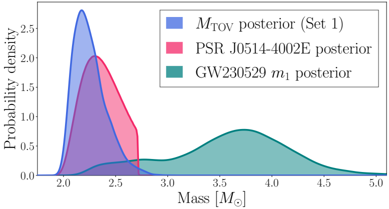

Object		Set 1	Set 2	Set 3
PSR J0514 -4002E	$m_{\rm PSR} > 1.17\,{\rm M}_\odot$	31%	34%	3.1%
	$m_{\rm PSR}$ unconstrained	24%	26%	1.9%
	$m_{\rm PSR} \in P^{\rm gal}(M_{\rm PSR})$	15%	8.1%	1.6%

$P(NS)$ for PSR J0514-4002E companion.

Other results – NICER model selection

Comparing hotspot models for NICER data from Ref. [6] (Ref. [26] below) and Ref. [7] (Ref. [17] below):

TABLE V: Posterior predictive ratios for the different M-R inferences of the NICER PSR J0030+0451 measurement. The ratio is given with respect to the original analysis of Ref. [26], i.e. the higher the value the more plausible the original analysis.

Ref.	Hot spot configuration	XMM used	Set 1*	Set 2*	Set 3*
[26]	ST+PST	×	1.0	1.0	1.0
[17]	PDT-U	×	1.18	1.15	1.16
	ST-U	×	2.05	2.98	2.99
	ST+PST	×	1.25	1.22	1.22
	ST+PDT	×	1.12	1.59	1.61
	ST-U	✓	7.62	8.15	8.41
	ST+PST	✓	20.67	22.27	23.31
	ST+PDT	✓	0.79	0.92	0.93
	PDT-U	✓	5.13	5.0	5.17

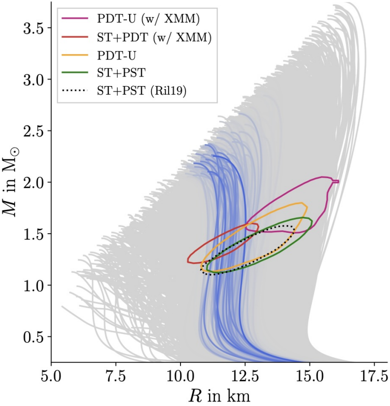

Other results – symmetry energy measurements

Comparing different measurements of the nuclear symmetry energy, CREX [8] and PREX [9] and the dipole measurement of $^{208}\mathrm{Pb}$ [10]

TABLE VI: Posterior predictive ratios of different symmetry energy measurements. The ratio is given with respect to CREX, i.e. the higher the value the more plausible is CREX vs. the measurement in the row.

Measurement	Set 1*	Set 2*	Set 3*
CREX	1.0	1.0	1.0
PREX-II	6.20	6.48	6.15
^{208}Pb dipole	2.02	2.14	1.95

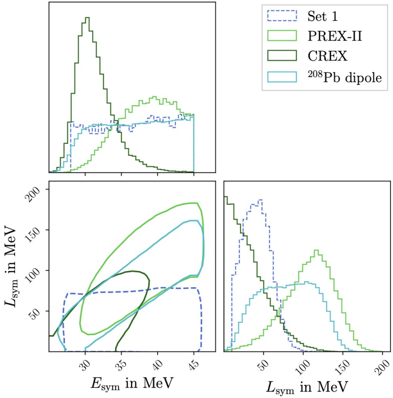

Conclusion

Nature of GW230529 primary:

- NMMA has compiled current EOS constraints into 3 sets (soon: with new NICER observation of PSR J0437-4715)
- $P(NS)$ ranges between $\sim 0.02\%$ to $\sim 17\%$ (depends on prior and spin)
- Results are still consistent with black hole interpretation

Other results:

- PSR J0514-4002E companion is most likely a black hole
- Model selection on NICER hotspots and symmetry energy measurements

References I

[1] "Observation of Gravitational Waves from the Coalescence of a $2.5 - 4.5\ M_\odot$ Compact Object and a Neutron Star". In: (Apr. 2024). arXiv: 2404.04248 [astro-ph.HE].

[2] Peter T. H. Pang et al. "An updated nuclear-physics and multi-messenger astrophysics framework for binary neutron star mergers". In: *Nature Commun.* 14.1 (2023), p. 8352. DOI: 10.1038/s41467-023-43932-6. arXiv: 2205.08513 [astro-ph.HE].

[3] Hauke Koehn et al. "An overview of existing and new nuclear and astrophysical constraints on the equation of state of neutron-rich dense matter". In: (Feb. 2024). arXiv: 2402.04172 [astro-ph.HE].

[4] Cosima Breu and Luciano Rezzolla. "Maximum mass, moment of inertia and compactness of relativistic stars". In: *Mon. Not. Roy. Astron. Soc.* 459.1 (2016), pp. 646–656. DOI: 10.1093/mnras/stw575. arXiv: 1601.06083 [gr-qc].

[5] Ewan D. Barr et al. "A pulsar in a binary with a compact object in the mass gap between neutron stars and black holes". In: *Science* 383.6680 (2024), pp. 275–279. DOI: 10.1126/science.adg3005. arXiv: 2401.09872 [astro-ph.HE].

[6] Thomas E. Riley et al. "A *NICER* View of PSR J0030+0451: Millisecond Pulsar Parameter Estimation". In: *Astrophys. J. Lett.* 887.1 (2019), p. L21. DOI: 10.3847/2041-8213/ab481c. arXiv: 1912.05702 [astro-ph.HE].

References II

[7] Serena Vinciguerra et al. "An Updated Mass–Radius Analysis of the 2017–2018 NICER Data Set of PSR J0030+0451". In: *Astrophys. J.* 961.1 (2024), p. 62. DOI: 10.3847/1538-4357/acfb83. arXiv: 2308.09469 [astro-ph.HE].

[8] D. Adhikari et al. "Precision Determination of the Neutral Weak Form Factor of Ca48". In: *Phys. Rev. Lett.* 129.4 (2022), p. 042501. DOI: 10.1103/PhysRevLett.129.042501. arXiv: 2205.11593 [nucl-ex].

[9] D. Adhikari et al. "Accurate Determination of the Neutron Skin Thickness of ^{208}Pb through Parity-Violation in Electron Scattering". In: *Phys. Rev. Lett.* 126.17 (2021), p. 172502. DOI: 10.1103/PhysRevLett.126.172502. arXiv: 2102.10767 [nucl-ex].

[10] A. Tamii et al. "Complete electric dipole response and the neutron skin in 208Pb". In: *Phys. Rev. Lett.* 107 (2011), p. 062502. DOI: 10.1103/PhysRevLett.107.062502. arXiv: 1104.5431 [nucl-ex].

APPENDIX

Population informed posterior

Posterior obtained with PDB prior:

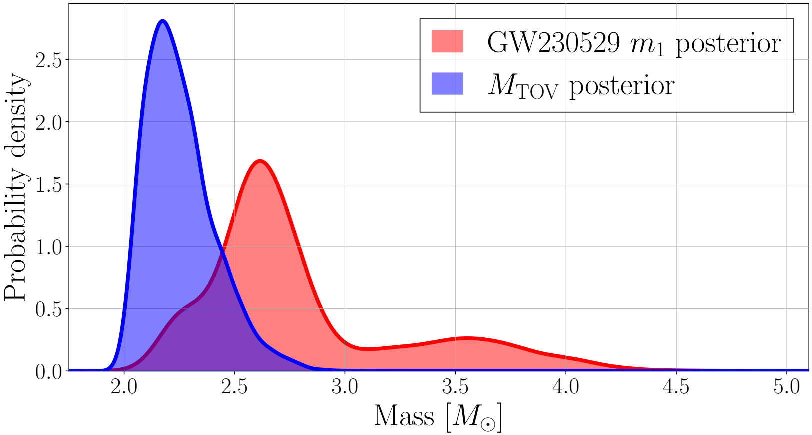

TOV mass posterior with set 3 (“Aggressive”)